MICROBIAL ECOLOGY

Microb Ecol (2003) 45:163–172
DOI: 10.1007/s00248-002-1028-x
© 2002 Springer-Verlag New York Inc.

Movement, Replication, and Emigration Rates of Individual Bacteria in a Biofilm

A.R. Rice,[1,4] M.A. Hamilton,[2,3] A.K. Camper[2,4]

[1] McLaughlin Engineers, Lakewood, CO, USA
[2] Center for Biofilm Engineering, Montana State University, Bozeman, MT 59717, USA
[3] Department of Mathematical Sciences, Montana State University, Bozeman, MT 59717, USA
[4] Department of Civil Engineering, Montana State University, Bozeman, MT 59717, USA

Received: 24 May 2002; Accepted: 3 September 2002; Online publication: 20 December 2002

ABSTRACT

Single-cell behavior within a biofilm was observed over a period of several hours. The observations were converted into quantitative stochastic rules governing the behavior of individual cells within a biofilm. Such a quantitative summary provides not only a concise description of the results but also information helpful when constructing computer models of dynamic biofilm systems. The time to division, emigration, and rate of motility of individual green fluorescent protein labeled *Pseudomonas aeruginosa* PAO1 cells in a 3–10 μm thick biofilm containing predominantly non-GFP labeled cells were calculated based on images of individual cells collected at 15-min time intervals. The biofilms were grown in flow cells and the images captured with a confocal laser microscope. Cells destined to emigrate are more active than those that remain; the geometric means for velocities in the biofilm are 1.0 μm/h for remaining cells and 1.5 μm/h for emigrating cells. The median time to emigration was 2.0 h. During the experimental observation period, the estimated probability for emigration is 0.44, illustrating that a substantial number of bacteria leave the field of view. Cells emigrate at a median time one-third that of the median time to replication. Specifically, the median time for cells to divide was 6.9 h, and it was estimated that 10% of the cells had a time to division greater than 10 h.

Introduction

In recent years, modeling of biofilm behavior and structure has been significantly advanced by application of the cellular automata approach. Cellular automata (CA) is a well-defined method [22] that has recently been used to create dynamic computer models for biofilms [1, 6, 11, 13, 14, 21]. The CA model simulates cell growth, detachment, and other biofilm processes based on rules that specify each cell's response to local environmental conditions within the biofilm. Typically, the rules governing chemical concentrations in the neighborhood of a bacterial cell are based on continuum representations, such as reaction and diffusion differential equations for the limiting substrate. In contrast, bacterial behavior, such as cell division, movement, and detachment, is modeled as discrete, sto-

Correspondence to: A.K. Camper; E-mail: anne_c@erc.montana.edu

chastic events. The numerical coefficients used in CA rules for bacterial cell division, movement, and detachment are often based on best guesses and extrapolation from measurements on the biofilm as a whole, rather than on experiments specifically designed to quantify single-cell behavior in the biofilm system being modeled.

Insight into single-cell behavior would be advantageous in the establishment of rules to be used for the stochastic events in biofilm formation. Although this type of information is limited, there are situations where observations have been taken. Movement of bacteria on surfaces has been documented where cells form dense microcolonies that then disperse in a matter of minutes [12]. Other experiments have shown that after replication of biofilm cells, daughter cells can spread out upon the surface, pack tightly near the parent cell location, be shed into the bulk fluid, roll along the substratum, or form long chains of cells [5, 7, 8, 15, 20]. It has been postulated that the various types of behavior exhibited by these cells are species dependent [8].

Although the above experiments provide insight into the behavior of individual cells, they were not designed to give quantitative information needed for models. There have been two instances where this level of detail has been obtained for biofilm formation by *Pseudomonas fluorescens*. Upon the initiation of biofilm formation, planktonic cells approach the surface and attach followed by rotational motion for up to half an hour with rotation gradually ceasing, resulting in a longitudinal irreversible attachment. Rotational behavior was also seen with detaching or emigrating cells that move to a nearby location and repeat the behavior of rotation and attachment. Subsequent to longitudinal attachment, cell division occurred resulting in two daughter cells 0.2 to 0.3 μm apart. After three to four generations, other movement was seen such as vibration, directional movement, and eventually emigration [9]. Further research into the development of *P. fluorescens* biofilms focused on the recolonization behavior of both motile and nonmotile emigrating cells. It was reported that the average recolonization distance for motile cells was 47 μm, which was 3 times greater than for nonmotile cells. This characteristic behavior allows for the redistribution of cells across a substratum to virtually all vacant spaces and is a key phase in the development of a confluent biofilm [7].

Another report of direct observation of growth and behavior of biofilm cells described four types of cell movement: packing, spreading, shedding and rolling [8]. This work involved the use of natural stream populations cultivated in flow cell reactors. The packing behavior arose from progeny cells remaining very close to the parent cell location and producing discrete, tightly packed microcolonies. Spreading of daughter cells by distances of 5–20 μm created diffuse microcolonies. Shedding behavior involved a parent cell being attached to the substratum while each daughter cell became oriented away from the substratum and detached upon the completion of division. Rolling cells maintained contact with the surface but were not stationary, nor did they form microcolonies. Exponential growth was observed in the microcolonies of the packing and spreading cells, but not for rolling or shedding cells. The authors state that these colonization maneuvers may be characteristics of individual species and can only be discerned by continuous observation.

A related report addressed growth of a marine bacterium (designated SW5 by the authors) on a surface-bound substrate [15]. Attached cells were observed to increase in size and then divide, with the two daughter cells moving away from each other. The cells tended to move great distances, up to 50 times their own length, before completing another division cycle. The migration rate was relatively slow with a mean of 0.15 μm/min. Detachment of cells from the substratum was also observed and postulated to be due to the depletion of sorbed nutrients.

A review of the literature demonstrated that there has been a lack of experiments specifically designed to procure the types of data needed to create the rules needed to simulate cell behavior in CA models. Although others have conducted similar research [8, 9, 15], the experiments were not designed to estimate rate coefficients for computer models. Consequently, the purpose of this paper is to present quantitative information on the growth, movement, and emigration of individual cells of *Pseudomonas aeruginosa* PA01 within a 3–10 μm thick biofilm in a parallel plate flow cell reactor as observed by confocal scanning laser microscopy. A cell was said to emigrate if it left the field of view; this is distinct from detachment since it is unknown whether the organisms entered the bulk fluid or simply moved along the surface to a new location outside of the field of view. Rates are calculated for replication, movement, and emigration of individual cells by tracking the position of specific cells and their progeny over the course the experiment. The analysis of movement velocities was based on two independent experiments.

Materials and Methods

Organism

A parent strain and a construct of *Pseudomonas aeruginosa* PA01 were used in this study. The parent strain contained a plasmid conveying resistance to 150 mg/L of carbenicillin. The construct strain contained the same plasmid, but production of a green fluorescent protein (GFP) was also encoded. The GFP was constitutively expressed, thus enabling each parent and daughter cell to be "self-labeling." The excitation wavelength of the GFP was 488 nm and the emission maximum was at 512 nm. These organisms were obtained from Dr. Mike Franklin at Montana State University. Cultures of the parent strain of the organism (PA01-GFP−) were kept separate from the GFP construct strain (PA01-GFP+) until the inoculation of the parallel plate flow cell reactor.

Stock cultures of both the parent strain and construct (PA01-GFP− and PA01-GFP+) were prepared by streaking for isolated colonies on R2A agar (Difco) that contained 150 mg/L of carbenicillin (Sigma). Isolated colonies were then transferred to fresh R2A/carbenicillin agar and incubated until a confluent lawn was present. The culture was harvested, placed in a 2% peptone–20% glycerol solution, and stored in 2.0-mL vials at −70°C. For each experiment, approximately 1.0 mL of frozen stock culture of each organism was used as an initial inoculum.

Media

The nutrient medium (K_2HPO_4, 0.7 g/L; KH_2HPO_4, 0.3 g/L; $(NH_4)_2SO_4$, 0.1 g/L; $MgSO_4 \cdot 7H_2O$, 0.01 g/L; glucose, 0.4 g/L) for each experiment was prepared as needed. The potassium salts, ammonium sulfate (Fisher), and reverse osmosis water were added to glass carboys; the containers were sealed and then autoclaved for 15 min per liter. The solution was cooled to room temperature before the remaining constituents were added. Proper amounts of glucose (Fisher) and magnesium sulfate (Aldrich) were dissolved in approximately 25 mL of reverse osmosis water and added to the solution via syringe and a 0.2-μm syringe filter.

Chemostat Operation

Two chemostat reactors were used to grow inocula for the experiments. The chemostats were operated at room temperature with a volume of 500 mL and a 5-h residence time (specific growth rate of 0.2/h, doubling time of 3.5 h). The cultures in the reactors were well mixed by a magnetic stir bar and plate and aerated by the laboratory pressurized air system and bacterial air vents (Gelman Sciences). After sterilizing all reactor components the system was assembled. Each reactor was filled with sterile nutrient medium described above, inoculated with 1.0 mL of the appropriate frozen stock culture (PA01-GFP− or PA01-GFP+), and operated in batch mode for 24 h. The pumps were then turned on to supply sterile medium to the reactors and the effluent was pumped to a waste container. The bacteria were grown in chemostats for 48 h, or about 10 residence times.

Flow Cell

Bacteria were observed on the wet side of the coverslip in a parallel-plate flow-cell reactor [17]. The entire flow-cell reactor system was set up on a laboratory cart to facilitate transportation to and from the microscope lab where the cell positions were recorded.

Cleaning of the flow cell prior to each experiment was carried out as follows. The polycarbonate base was submersed in 95% ethanol for 30 min and then subjected to UV light for 30 min. Each experiment utilized a new glass coverslip that was washed twice with antibacterial soap and rinsed twice with 95% ethanol. The coverslip was then autoclaved for 20 min and dried at 115°C for 24 h. Other assorted materials (tubing, coverplate, gasket, screw, and nuts) were autoclaved for 20 min. After all parts of the flow cell were sterilized or cleaned, the flow cell was assembled inside a biological hood. The tubing upstream from each of the reactors was replaced for each experiment.

Prior to inoculation, the flow cell and all upstream tubing were filled with sterile medium to purge air from the system. Using a sterile syringe, 20 mL of parent strain inoculum (PA01-GFP−) was withdrawn from a 48-h chemostat culture and placed into the inoculation vessel along with 0.5 ml of PA01-GFP+ to give a ratio of approximately 100:1 GFP− to GFP+. The inoculum was rapidly mixed using a magnetic stir bar and plate to break up cell clumps.

The entire volume of the stirred inoculum was pumped through the flow cell in a series of three pulses. Approximately one-third of the inoculum (7.0 ml) was drawn through the flow cell and flow was stopped for 5 min. The second and final 7.0 mL was pumped in a similar manner, with 5-min stagnation periods before resuming flow. This method of introducing cells into the reactor was used to ensure that high initial cell densities on the coverslip were reached.

After the entire volume of inoculum had passed through the reactor and the final 5-min no-flow period expired, flow of sterile, cell-free medium commenced. The flow rate was set at 2.0 mL/min, producing laminar flow ($Re \sim 5.5$) in the reactor's channel of 12 mm × 1.5 mm cross section and 37 mm length.

Imaging

A field of view with single, isolated GFP cells was chosen at the onset of the experiment and the location of individual bacterial cells was tracked via fluorescence emitted from the GFP at discrete time points. Imaging commenced 24 h after inoculation and continued at 15-min intervals for 10.5–11 h. TIF format images of PA01-GFP+ cells were produced using a Leica TCS-NT confocal microscope system. Excitation of the protein was achieved with the 488-nm laser light source. The fluorescent emission, maximum at 512 nm, was registered after passing through a BF filter

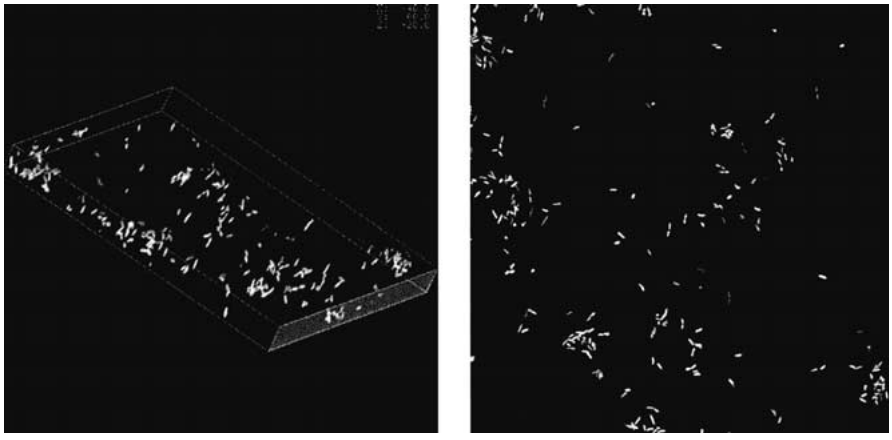


Fig. 1. Example 3D and 2D images of GFP cells in a biofilm composed of GFP and nonlabeled *Pseudomonas aeruginosa*. Left image is a rotated, three-dimensional compilation and right imageis a composite, top-down view of the same three-dimensional image composed of 18 separate 2D optical slices. Dimensions of box in left image: 100 × 100 × 18.5 μm; distortion in one dimension is due to differences in pixel density per micron. Dimensions of right image: 100 × 100 μm. Note that only GFP-labeled cells are visible in this image.

block with a cutoff above and below 500 and 550 nm, respectively. PA01-GFP− organisms were also present in the reactor, but were not visible because of the absence of GFP. The original ratio of approximately 100 GFP− to 1 GFP+ cells was seen to be maintained throughout the experiment by periodic examination of light microscopy images and estimation of total cell numbers compared to those that were fluorescent (data not shown).

Since it is known that exposure to laser light at high intensity from a scanning confocal microscope can damage bacterial cells [2], precautions were taken to minimize exposure of the bacteria to laser light. At each interval, the desired field of view was first checked for focus by eye with transmitted white light. Subsequently, the image was captured using the laser light source. This method greatly reduced the amount of time the sample was subjected to bleaching and heating from exposure to the laser beam. In addition, the lowest possible laser power setting was used, typically 50%, to minimize exposure of the biofilm to the laser.

Images were acquired at ∼0.5-μm elevation intervals starting at, and proceeding away from, the wet surface of the coverslip. These optical slices were compiled to produce a three-dimensional picture of GFP-labeled cells within the biofilm matrix composed of both labeled and nonlabeled bacteria using software provided by Leica. A composite image, or "top-down view," of GFP images from each elevation at one time point was also stored in TIF format (Fig. 1).

The stored images were then subjected to analysis. Extracting the *x*, *y*, *z* coordinates of the centroid of cell in the images was undertaken in two steps. The first step required that individual cells be uniquely identified and the two-dimensional *x*, *y* coordinates of each cell be determined. The second step produced the third, or *z*, coordinate of each cell.

To determine *x*, *y* coordinates of each cell, the composite image files were imported into an image analysis software package, Image-Pro Plus, Version 3.00.00 (Media Cybernetics). The software was calibrated based on the actual dimensions (100 μm × 100 μm for images captured using 100×, 1.4 NA, oil immersion objective) of each image. The auto-count feature was set to identify all objects (cells) within a specified area range, usually 0.5 to 2.5 μm^2. The software automatically assigned each cell an object number, and *x* and *y* centroid coordinates, in micrometers, with the origin being the upper left corner of the image. Occasionally, several cells were contiguous and had to be manually tagged. In this event, the software still recorded the *x*, *y* coordinates of the object; however, it was the researcher's task to identify and tag the locations of each of the contiguous cells.

To determine the *z* coordinate of each cell, all the images in a particular stack were examined. An elevation of zero was assigned to the image nearest the location of the substratum. Each cell was in focus in a minimum of two adjacent images and it was therefore necessary to determine which image best reflected the location of the centroid of each cell. The absolute elevation of each cell was based on the image number in the stack and the distance between images.

Because the microscope stage moved laterally by small amounts during the course of each experiment, the magnitude and direction of the image shifts were determined and used to make mathematical corrections to the centroid coordinates. The shifts were determined by visually aligning a fixed landmark in two consecutive images and measuring the (*x*, *y*, *z*) shift in the origin in the second image required to accomplish that alignment. This shift provided a single correction that was applied to each object in the second image. This technique was then applied sequentially to each consecutive pair of images.

The result of the image analysis process was a list of cells for each particular image containing the software-assigned object number and *x*, *y*, and *z* (corrected) centroid coordinates. An example of this is shown in Table 1; the microscope stage vertical step size and coordinate dimensions are in micrometers. The next step was to assign each cell a unique identification (i.e., A, B, C...) and then determine which cell/object number (i.e., 1, 2, 3...) from each image corresponded to that ID. The result was a chart such as that of Table 2. Consider for example the cell with ID=C in Table 2. It was object 2 in images 0–3, object 3 in images 4–7, and object 4 in images 8–11. After the associations between cells and objects numbers were tabulated, each table was imported into Microsoft Access 97 from Microsoft Excel 97. The data were then sorted first by cell ID and second by time.

Statistical Methods

The quantitative summaries acquired from the observations and images include the distribution of movement distances for emi-

Table 1. Bacterial cell object numbers and corrected coordinates of the centroids[a]

Object	Centroid		
	x	*y*	*z*
1	51.95	46.26	0.49
2	51.78	48.17	0.61
3	53.16	48.47	0.49
4	54.46	49.18	0.49
6	52.57	52.41	0.61
7	56.79	53.46	0.85
8	53.57	53.75	0.61
T1	50.24	50.63	0.97
T2	51.61	50.14	0.49
T3	53.76	50.04	1.46
T4	53.67	50.73	0.61
T5	52.59	51.31	0.61
T6	52.59	51.02	2.43

[a] For this image, the vertical step size was 0.486 μm. The centroids are expressed in distance (μm) from the origin, which was the upper left-hand corner of the field of view at the substratum. The T code indicates that, either in this image or an earlier image, the bacterial cell was coded manually by the microscopist when two contiguous cells were mistakenly identified as one large cell by the image analysis software and the microscopist manually split apart the two cells. Because the image analysis software arbitrarily assigned object numbers, the same cell may be assigned different object numbers in different images. See Table 2 for a chart that tracks the object numbers for each cell. This table corresponds to Image 1 in Table 2.

grating (moving out of the field of view) and remaining cells (those that were present throughout the observational time period), the probability of emigration following a division event, the distribution of time to emigration, and the distribution of time to division. These distributions and probabilities can be used to create CA rules governing individual stochastic cell events during biofilm development when constructing a computer model.

For the movement distance distribution, an individual bacterium was tracked with time and its centroid position was recorded at each time point. Table 3 demonstrates the results for one cell (labeled cell C) for the first dozen time points. From such data, the Euclidean distance each cell moved between adjacent observation times was determined and expressed as velocity (μm/h). Cells that emigrated during the experiment were analyzed separately from those that remained in the field of view throughout the whole observation period. The velocities were then sorted from least to greatest, and the cumulative percentage plotted separately for emigrating and remaining cells. To determine the repeatability of the results, a random effects analysis of variance was conducted separately for the emigrating and remaining groups of cells. The response was the log-transformed velocity and the random effects were experiments, cells (nested in experiment for each of the two experiments), and measurement error (within cell log velocity deviations).

When tracking the individual cells, the time at which a cell emigrated or divided was recorded. The occurrence of these events was determined manually and confirmed by assembling the images into a short movie covering the time of the event. From this information the cumulative percentage plots could be created. A large portion of the observed times either began before or continued past the period of observation. For example, when a cell was in the field of view at the start of the observations period and divided at 4 h, we knew that it was at least 4 h since the last time the cell divided; thus we had a lower bound on the time to division, but not the exact time. In statistical textbooks and computer packages, such an observation is said to be "censored." We used the nonparametric procedure known as the Kaplan–Meier method for analyzing censored data to estimate the cumulative percentage curve [10]. The cumulative percentage plot

Table 2. Typical table created to track the object number in each image that is the same cell[a]

Image:	0	1	2	3	4	5	6	7	8	9	10	11
Time (min):	0	13	26	43	58	72	88	103	118	133	148	163
Cell ID	Object numbers											
A	1	1	1	1	1	1	1	1	1	1	1	1
C	2	2	2	2	3	3	3	3	4	4	4	4
E	3	3	3	3	2	2	2	2	2	3	3	3
G		4	4	T7	4	5	4	4	3	2	2	2
I	5	6	6	5	6	9	10	8	9	T7	10	10
K			7	6	7	10	11	9	10	9	11	11
M	6	7	8	8	9	−1	−1	−1	−1	−1	−1	−1
N	7	8	9	7	8	11	12	10	11	10	12	12
O	T1	T1	T1	T1	T1	7	8	6	7	8	9	8
Q	T2	T2	T2	T2	T2	T1	T1	T1	T1	T1	6	6
S	T3	T6	T5	T3	T6	T5	T5	T5	T5	T6	T5	T6
W	T4	T3	T3	T6	T3	T2	T2	T2	5	5	5	5
Z	T5	T4	T4	T5	T4	T3	T3	T3	T3	T3	T3	T3
AB	T6	T5	T6	T4	T4	T4	T4	T4	T4	T5	T4	T5

[a] The image analysis software assigned the object numbers to bacteria cells. Just the first 12 images and only 14 cells are shown in this table. T denotes manual assignment of an object number, −1 denotes that a cell emigrated prior to that image, and a blank denotes a bacterial cell that will first appear as a daughter cell later.

Table 3. The times of observation, corrected coordinates of the centroids of the bacterial cell C, and velocity[a]

Cell ID	Image	Time (min)	Object number	x	y	z	Velocity (μm/h)
C	0	0	2	51.67	48.11	0.61	NC
C	1	13	2	51.78	48.17	0.61	0.59
C	2	26	2	51.81	48.04	0.61	0.63
C	3	43	2	51.70	48.13	0.49	0.65
C	4	58	3	51.63	48.15	0.49	0.29
C	5	72	3	51.63	48.32	0.49	0.73
C	6	88	3	51.57	48.28	0.73	0.94
C	7	103	3	51.44	48.15	0.85	0.88
C	8	118	4	51.49	48.21	0.73	0.58
C	9	133	4	51.40	48.13	0.24	2.02
C	10	148	4	50.99	48.09	0.73	2.56
C	11	163	4	50.99	48.14	0.97	0.98

[a] Only the first 12 images are presented. Coordinates are defined as in Table 1. Velocity is the distance (μm) that the cell's centroid moved from the previous position divided by the number of minutes in the interval since the previous observation, then multiplied by 60 min/h. NC denotes not calculable because the previous position was not observed. This table was created using the image number and object number information as in Table 2. Cell C was in the remaining cell group.

and a band showing the 95% confidence interval any percentile were plotted for both time to emigration and time to division. The median time was calculated from each plot. The statistical calculations and graphics were done with the Minitab statistical software package (Release 13; see the Web site http://www.minitab.com).

The analysis of time to emigration and time to division was performed for only one of the two experiments. In that experiment, four fields of view were visited at each observation time. Data from the four fields of view were combined for the analysis. The confidence interval bands around the cumulative percentage plots account only for within-experiment variation.

Results

Cell Movement

The cumulative percentage plots for remaining and emigrating cell velocities are shown in Fig. 2. The descriptive statistics for both cell types are listed in Table 4. Both experiments showed greater movement for emigrating cells relative to remaining cells. The two means in Table 4 are statistically significantly different (two-tailed p-value < 0.005). The geometric means (antilogs of the means in Table 4) are 1.0 μm/h for remaining cells and 1.5 μm/h for emigrating cells. The 80th percentiles of the cell velocities for remaining and emigrating bacteria were 2.0 and 3.7 μm/h, respectively, which are statistically significantly different (two-tailed p-value < 0.01). The 90th percentiles of the cell velocities for remaining and emigrating bacteria were 3.0 and 5.8 μm/h, respectively, which are statistically significantly different (two-tailed p-value < 0.01).

The repeatability standard deviation, which is the square root of the total variance for a single, randomly chosen $\log_{10}$ velocity, was 0.41 for remaining cells and 0.46 for emigrating cells. The $\log_{10}$ velocities were repeatable in the sense that the between-experiments component of variance was negligible. The component of variance for cells within an experiment was statistically significant ($p < 0.001$), contributing 16% of the total variance for remaining cells and 27% of the total variance for emigrating cells. The main contributions to the total variance, 84% for remaining cells and 73% for emigrating cells, were the combined, not statistically separable effects of sporadic movement of an individual cell and the random errors involved in measuring the velocity during different time intervals.

Cell Emigration

Figure 3 is the cumulative percentage plot for the time to emigration for the 34 cells that emigrated. The median time to emigration was 2.0 h. Even though cells left the field of view, direct observation indicated that there were no new cells recruited at the points of observation during the duplicate experiments.

During the period of observation, 0.44 of all observed cells emigrated. Note that additional cells may have emigrated after the observation period ended.

Cell Division

Figure 4 shows the cumulative percentage plot of the time to division. The median time for cells to divide was 6.9 h,

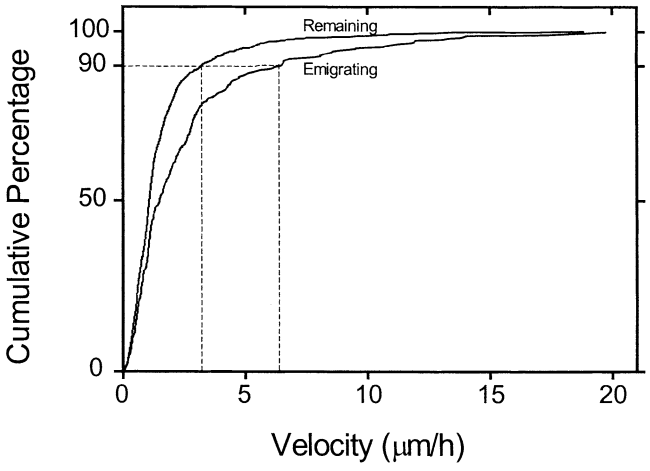


Fig. 2. Cumulative percentage plot of the distribution of cell velocities for both remaining and emigrating cell groups. The dashed lines show that the 90th percentile for emigrating cells is almost twice the 90th percentile for remaining cells.

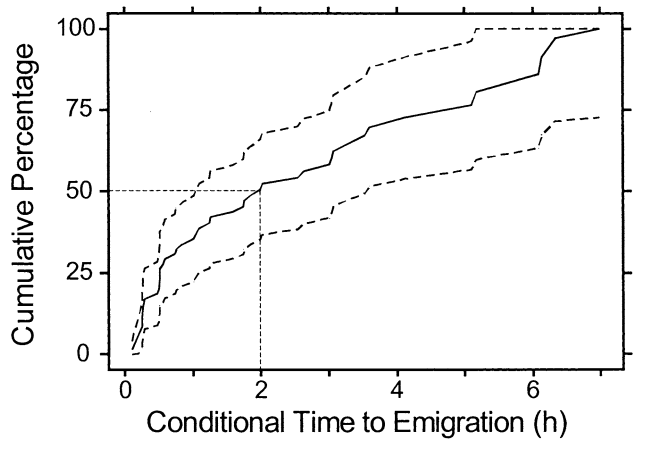


Fig. 3. Cumulative percentage plot showing the distribution of time to emigration for cells that will emigrate within 6.5 h. Dashed lines represent 95% confidence interval for the cumulative percentage. The median time to emigration of 2 h is indicated by the dotted lines. The cumulative percentage was estimated by the Kaplan–Meier method using observations on 166 bacterial cells, of which 118 provided censored times. The plots are based on the estimate that 44% of daughter cells will emigrate prior to dividing within 6.5 h.

with 90% of the organisms having divided within approximately 10 h. It is anticipated that if the observation time had been extended, all viable cells would have eventually divided. However, because those long times to division were not observed, the cumulative percentage plot of Fig. 4 could not be extended all the way to 100%. It is of interest to note that this median time to division is somewhat slower than what was observed in the chemostat used to prepare the inoculum for the flow cell (division time of 3.5 h).

Discussion

In order for CA modeling efforts to advance, there is a clear need for data that can be used to describe the behavior of individual cells within a biofilm. These models may then be used to make predictions on biofilm responses to varying conditions and subsequently verified by experimentation. The information presented here provides a framework for obtainin quantitative descriptions of cell behavior in regard to emigration, time to division, and mobility within an established biofilm. The methods used could be applied to biofilms of virtually any organism grown over a variety of time frames, under differing nutrient conditions and flow regimes.

Under the conditions of these experiments, *Pseudomonas aeruginosa* cells within the biofilm exhibited a median observed time to division of 6.9 h, corresponding to a specific growth rate of 0.10 h^{-1}. This specific growth rate is identical to the value obtained in similar experiments with the same organism in a day-old biofilm [16]. It is important to note that the mean time to division cannot be held constant throughout biofilm development. As shown by Rice et al. [17], *P. aeruginosa* had an extended lag time immediately after attachment, with only 7% of the organisms replicating in the first 12 h. Once these cells had resumed growth, the above-noted specific growth rate of

Table 4. Summary statistics for the $\log_{10}$ velocities (μm/h)[a]

						Variance Component (% of total variance)		
Cell type	Nc	Ni	Mean	SEM	Repeatability SD	Experiment	Cell	Interval
Remaining	47	1659	0.02	0.025	0.41	0.00 (0%)	0.03 (16%)	0.14 (84%)
Emigrating	34	287	0.18	0.047	0.46	0.00 (0%)	0.06 (27%)	0.16 (73%)

[a] Nc denotes the number of cells observed, Ni denotes the total number of time intervals for which velocity was measured, SEM denotes the standard error of the mean, and SD denotes the standard deviation.

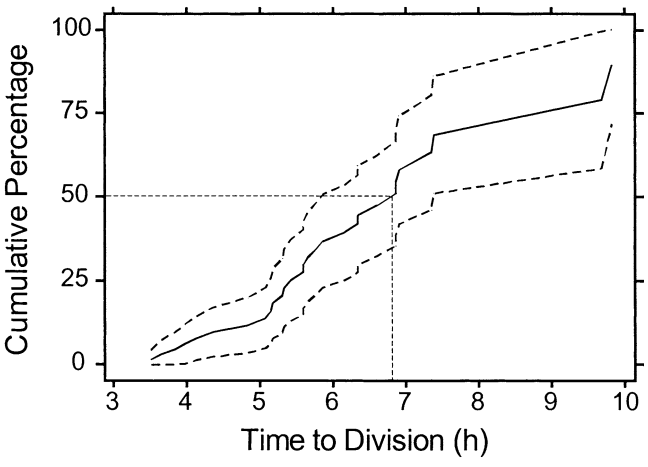


Fig. 4. Cumulative percentage plot showing the distribution of time to cell division. Dashed lines show the 95% confidence interval for the cumulative percentage. The median of 6.9 h is indicated by the dotted lines. The cumulative percentage was estimated by the Kaplan–Meier method using observations on 166 bacterial cells, of which 137 provided censored times.

0.1 h^{-1} was attained. It was also interesting to note that during this lag period, 21% of the population emigrated; once cell division had commenced, emigration increased to 45%.

The cumulative distributions compiled for both the emigrating and remaining cells show that these cells, although growing in a 3–10 μm thick biofilm, are still quite active in terms of movement. Although we did not attempt to calculate and analyze the direction vectors of cell movement, it was our casual observation that the cells exhibited a random walk with no discernable net movement in a specific direction. The distributions show that there are two subpopulations, with the emigrating cells being significantly more dynamic than the cells that remain in the field of view. Even so, the remaining cells exhibited a typical velocity of 1 μm/h, which expands to 24 μm/24 h, a substantial distance if the movement is through the polymeric substances that fix the cells to the surface. This movement was even more pronounced for bacteria that eventually left the field of view, with the 90th percentile rate being 5.8 μm/h. It is suspected that the difference in movement between the two subpopulations is even more striking than what these results indicate. Undoubtedly, some of the cells designated as "remaining" emigrated at some point after the experiment ended based on the behavior evidenced by their predecessors. However, their movement was grouped with the "remaining" cells for lack of an alternative, which would inflate the velocity for this group of cells overall. From these results, it is concluded that cells destined to emigrate display significantly more motion than those destined to remain in the biofilm.

The estimated probability that a cell emigrates is 44%. These results suggest that emigration with *P. aeruginosa* PA01 is a significant event in biofilm development, with the dislocation of approximately a third of new cells from their point of origin out of the field of view at a median time of 2.0 h. During the time frame of the experiments described herein, there was no significant microcolony development with respect to daughter cells being located in close proximity to parent cell location. The spreading behavior persists into a maturing biofilm, although likely hindered by the biofilm matrix. This behavior also contributes to a rather flat, uniform biofilm structure during the early stages of accumulation. These results tend to support to the finding by O'Toole and Kolter [12] that microcolonies of *P. aeruginosa* develop as result of recruitment and not by lineage of cellular division.

Although the literature has no similar studies where the emigration of the two subpopulations (emigrating and remaining) has been examined, others have noted the movement of bacterial cells on surfaces. In biofilms of *Pseudomonas* JD8 that were less than a monolayer in thickness, cells moved distances of up to 150 μm before completion of a division cycle. The average velocity was 9.0 μm/h [15]. In a study examining the replication patterns of various biofilm organisms from a natural stream population, the same behavior was seen [8]. Dalton et al. [5] also report that in a multilayered biofilm, daughter cells of a marine bacterium appeared to displace neighbors to gain access to the substratum or were lost to the field of view.

There is evidence to suggest that there is a physiological basis for the cell behavior seen in these studies. Sauer et al. [19] showed that there was activation of the *las* regulon, loss of motility, and a change in regulation of over 50 proteins in *P. aeruginosa* within approximately 24 h of attachment in a flowing system. These proteins included those responsible for metabolic processes, lipid biosynthesis, and molecular transport, and those involved in adaptation and protection of the organism. During the same study, there was a marked increase in motility of individual cells prior to wholesale migration out of the biofilm. This difference in motility was also observed for *Pseudomonas putida,* where there was a change from flagellar motility to type IV pili-based twitching motility 12 h

after attachment. After 3 days, the flagellar proteins were once again detected [18]. In the same experiments, there was a change in protein expression patterns as determined by 2-D gel electrophoresis as soon as 4 h after initial attachment that progressed over a 24-h observation period.

Others have noted specific physiological differences between suspended and attached cells. Prigent-Combarent et al. [16] demonstrated that biofilm formation resulted in the differential expression of genes involved in extracellular polymeric substance (EPS) production, osmolarity, oxygen limitation, cell–cell signaling, and motility in *Escherichia coli* K12. Davies and Geesey [3] and Davies et al. [4] showed that the gene *algC*, which is responsible for lipopolysaccharide core biosynthesis and the production of alginate, was upregulated upon attachment of *P. aeruginosa*.

To illustrate the manner in which rates of movement of bacterial cells, the time to division or emigration of a cell, and the probability of a cell to emigrate can be used in cellular automata models of biofilm growth, two examples are provided. In the first case, the rates provided by the experiments would be used to create a simulation using rules chosen from the data. In this simulation, at the time a cell divides, the daughter cell would be randomly identified as an emigrating cell or a remaining cell, with the probability of emigration set at 0.40. The time of emigration could be randomly chosen based on (a smooth approximation of) the distribution of Fig. 2. If the substrate concentration and biofilm thickness are similar to those used in the experiments used to create the data, the cell could also be assigned a random division time based on the distribution in Fig. 3. If the randomly chosen cell division time is less than the emigration time, the cell will divide at the chosen time and the daughter will be modeled with the same rules.

A second example would be to use the data to create rules to evaluate other models. For example, some existing cellular automata models employ rules that force cells to move when there is a high density of bacteria in their neighborhood [14]. In this case, the existing model could have input parameters set to simulate the conditions used in the experiments described in this manuscript. A simulation would then be run, with the movements of the individual remaining bacteria recorded. The velocities and the distribution of the log velocities would then be calculated. The evaluation would be comparisons of the model's cell velocity distribution and statistics to those in Fig. 2 and Table 4.

Both of these examples demonstrate the usefulness of rate data in establishing rules for CA biofilm models. The results of this paper are only a beginning in the establishment of these rules; similar experiments should be done for a variety of organisms under a number of conditions to assess how universal biofilm phenomena actually are and how relevant model predictions will be.

Acknowledgments

This work was conducted at the Center for Biofilm Engineering, an NSF Engineering Research Center, through cooperative agreement EEC-8907039. Funding for the confocal microscope was provided by the NSF through agreement BES-9724353. The authors thank Mr. John Neuman for his assistance in the laboratory.

References

1. Colasanti R (1992) Cellular automata models of microbial colonies. Binary 4:191–193
2. Caldwell DE, Korber DR, Lawrence JR (1992) Imaging of bacterial cells by fluorescence exclusion using scanning confocal laser microscopy. J Microbiol Methods 15:249–261
3. Davies DG, Geesey GG (1995) Regulation of the alginate biosynthesis gene *algC* in *Pseudomonas aeruginosa* during biofilm development in continuous culture. Appl Environ Microbiol 61:860–867
4. Davies DG, Chakrabarty AM, Geesey CG (1993) Exopolysaccharide production in biofilms: Substratum activation of alginate gene expression by *Pseudomonas aeruginosa*. Appl Environ Microbiol 59:1181–1186
5. Dalton HM, Poulson LK, Halasz P, Angles ML, Goodman KE, Marshal KE (1994) Substratum-induced morphological changes in a marine bacterium and their relevance to biofilm structure. J Bacteriol 176:6900–6906
6. Hermanowicz SW (1999) Two-dimensional simulations of biofilm development: effects of external environmental conditions. Water Sci Technol 39 (7):107–114
7. Korber DR, Lawrence JR, Sutton B, Caldwell D (1989) Effect of laminar flow velocity on the kinetics of surface recolonization by Mot+ and Mot− *Pseudomonas fluorescens*. Microb Ecol 18:1–19
8. Lawrence JR, Caldwell DE (1987) Behavior of bacterial stream populations within the hydrodynamic boundary layers of surface microenvironments. Microb Ecol 14:15–27
9. Lawrence JR, Delaquis PJ, Korber DR, Caldwell DE (1987) Behavior of *Pseudomonas fluorescens* within the hydrodynamic boundary layers of surface microenvironments. Microb Ecol 14:1–14

10. Lee ET (1992) Statistical Methods for Survival Data Analysis, 2nd ed. Wiley, New York
11. Noguera DR, Pizarro G, Stahl DA, Rittmann BE (1999) Simulation of multispecies biofilm development in three dimensions. Water Sci Technol 39:123–130
12. O'Toole GA, Kolter R (1998) Flagellar and twitching motility are necessary for *Pseudomonas aeruginosa* biofilm development. Mol Microb 30:295–304
13. Picioreanu C, van Loosdrecht MCM, Heijnen JJ (1997) Modelling the effect of oxygen concentration on nitrite accumulation in a biofilm airlift suspension reactor. Water Sci Technol 36(1):147–156
14. Picioreanu C, van Loosdrecht MCM, Heijnen JJ (2001) Two-dimensional model of biofilm detachment caused by internal stress from liquid flow. Biotechnol Bioeng 72:205–218
15. Power K, Marshall KC (1988) Cellular growth and reproduction of marine bacteria on surface-bound substrate. Biofouling 1:163–174
16. Prigent-Combarent C, Vidal O, Dorel C, Lejeune P (1999) Abiotic surface sensing and biofilm-dependent regulation of gene expression in *Escherichia coli*. J Bacteriol 181:5993–6002
17. Rice A, Hamilton MA, Camper AK (2000) Apparent surface associated lag time in growth of primary biofilm cells. Microb Ecol 40:8–15
18. Sauer K, Camper AK (2001) Characterization of phenotypic changes in *Pseudomonas putida* in response to surface-associated growth. J Bacteriol 183:6579–6589
19. Sauer K, Camper AK, Ehrlich GD, Costerton JW, Davies DG (2002) *Pseudomonas aeruginosa* displays multiple phenotypes during development as a biofilm. J Bacteriol 184:1140–1154
20. Shapiro JA, Hsu C (1989) *Escherichia coli* K-12 cell–cell interactions seen by time-lapse video. J Bacteriol 171:5963–5974
21. Wimpenny JWT, Colasanti R (1997) A unifying hypothesis for the structure of microbial biofilms based on cellular automaton models. FEMS Microbiol Ecol 11:1–6
22. Wuenshce A (1998) Classifying cellular automata automatically. Santa Fe Institute working paper 98-02-018